ISSN 1392–1320 MATERIALS SCIENCE (MEDŽIAGOTYRA). Vol. 12, No. 3. 2006

Factual Revelation of Correlation Lengths Hierarchy in Micro- and Nanostructures by Scanning Probe Microscopy Data

Grigory Valentinovich VSTOVSKY

N. N. Semenov Institute of Chemical Physics, RAS, 4 Kosygin Street, 119991, Moscow, Russia

Received 03 November 2005; accepted 16 March 2006

A new method is proposed to reveal the characteristic scales of substructures (in the case if they are present) in surface structure represented by scanning probe microscopy (SPM) data. The method is based on processing the structural functions (SF) of surface relief profiles to determine the positions of maxima of SF's negative second derivative. New approach is checked on model SFs, model structures and real SPM data (on LiF dissolution surfaces, track-etched membranes and shungite rocks). It is shown that the positions correspond to the characteristic scales, or correlation lengths, that can be related to objects having geometrical or physical sense. The use of the set of correlation lengths instead of one effective length makes it possible to analyze in details a hierarchical structure of the objects under study. This is extremely important when investigating the objects with complex many level hierarchical structures that are the natural structures, structures of composite materials etc.

Keywords: scanning probe microscopy; structural function; correlation length; persistency length; flicker noise spectroscopy.

INTRODUCTION

Fast prevalence of scanning probe microscopy (SPM) during last decade stimulates exploration of new possibilities of quantitative description (parameterization) of data obtained by SPM as nowadays the analysis of such data reduces mostly to description (qualitative and quantitative) of characteristic elements of micro and nanostructures which can be interpreted in geometrical (circles, chains, dendrites, etc.) or special (phase boundaries, grains, lamellae, etc.) terms [1]. However, modern standard of SPM apparatus enables to obtain reliable data about physical characteristics with chaotic (at the first glance) surface distributions. Parameterization of such data remains the issue of the day. Solution of the problem will push forward the new approaches to analysis and preselection of SPM data, the use of the data in investigations of irregular chaotic structures, control of technological processes, etc. Among the many works on the subject using different approaches [2] some later works [3 – 7] were based on the use of Flicker-Noise Spectroscopy (FNS) describing chaotic structures in terms of correlation lengths and rates of correlation losses. This work can be considered as resumption of these investigations on the base of more detailed analysis of structural functions (SF) of surface relief profiles. First we describe the present and new procedures of correlation lengths determination then describe the applications to real SPM data (on LiF dissolution surfaces, track-etched membranes and shungite rocks). Much attention is paid in Appendix C to model examples to make the readers sure that parameters determined by new method have some definite physical sense depending on the system under study.

*Corresponding author. Tel.: +7-495-9397395; fax.: +7-495-9397501.
E-mail address: *vstovsky@polymer.chph.ras.ru* (G.V. Vstovsky)

PARAMETERIZATION OF SFs IN FNS

SFs provide a very effective instrument of theoretical and numerical investigations of chaotic systems and processes, for instance, a turbulence [8]. FNS method [3 – 7, 9, 10] as applied to processing of temporal and spatial series (digital sequences of numbers with some sampling step) consists of calculation of SFs (difference moments) and power spectra that are parameterized then on the base of non-linear model trends. Here we focus only on SFs of surface profiles. SF of order p is calculated for the profiles of surface $h(x,y)$ along one of the directions (x, for example) by the formula

$$\Phi^p(\Delta) = \frac{1}{M}\sum_{k=1}^{M}\left|h(x_k) - h(x_k+\Delta)\right|^p , \qquad (1)$$

where $M = N - \Delta/\Delta x$, Δ is an SF lag, $h(x)$ is the profile height given discretely at the points $x_k = k\Delta x$ (Δx is the sampling step) along x direction for some profile disposition y, N is the overall number of points of the profile. Typical view of SF is shown in Fig. 1.

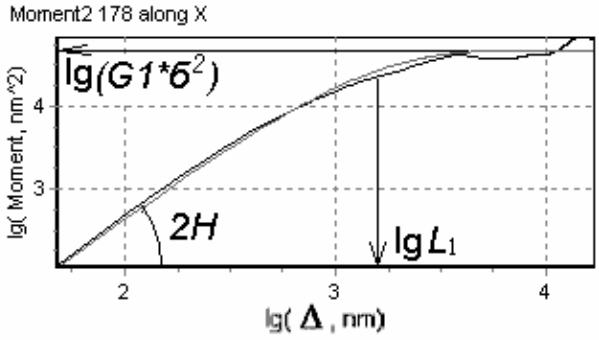

Fig. 1. Typical view and parameterization scheme of SF of the second order, see Appendix A (algorithm A1). "Moment2" (difference moment) is for SF of the second order

A physical sense of such a dependence is that the growth of SF with increase in lag Δ for the small Δ means

a presence of some correlation interrelations in the structure of surface (presented by its profile). Saturation of SF with increase in lag Δ means a loss (decay) of the correlation links. The conditional boundary L_1 of these ranges determined in one or another way (by one or another algorithm) gives evaluation of a so called correlation length (CL) – a characteristic size of surface regions within which there are the correlation links in the chaotic surface structure. Hurst parameter H characterizes a rate of correlation decay. Parameterization procedure used in [4 – 7] is described in Appendix A in details. Invention of this procedure has made it possible to conduct a computer based parameterization of chaotic reliefs automatically by unique scheme [4 – 7].

It should be stressed that a term "correlation length" was introduced [3, 8 – 10] by its physical sense for chaotic spatial ("correlation length") or temporal ("correlation time"), and other series having continuous power spectrum. In the case of model structures, see Appendix C, or presence (in the real structure) of the objects that can be interpreted in geometrical terms, the term "correlation length" should be replaced by something like the "size of coherency region" or 'persistency length'.

The peculiarity of "two dimensional" objects such as surface relief is that they consist of great number of series in two independent directions. For handling such object the original procedure was developed [4] which is as follows. A given number (for example, 100) profiles in the same direction was randomly picked up from each relief. Their parameterization can be done in two ways. The first one is to calculate SF parameters for each profile and then to average them for each relief. The second is to calculate mean SF for each profile and then to determine its parameters. The second way is more convenient. The parameters values changed by (2 – 5) % for increase in number of randomly picked up profiles from 20 to 100. This value can be thought of as the accuracy of the parameters obtained.

In the simplest case in Fig. 1 SF has one "step" only. SF in Fig. 2, a, below has two "steps" that implies a presence of two different imposed substructures of different scales. Determination of their characteristic CLs by unique algorithm of SPM data processing on the base of parametric approximation is a very complex problem. Next we propose a procedure of evaluation of CLs for the cases of two and more substructures (the "steps") of SF.

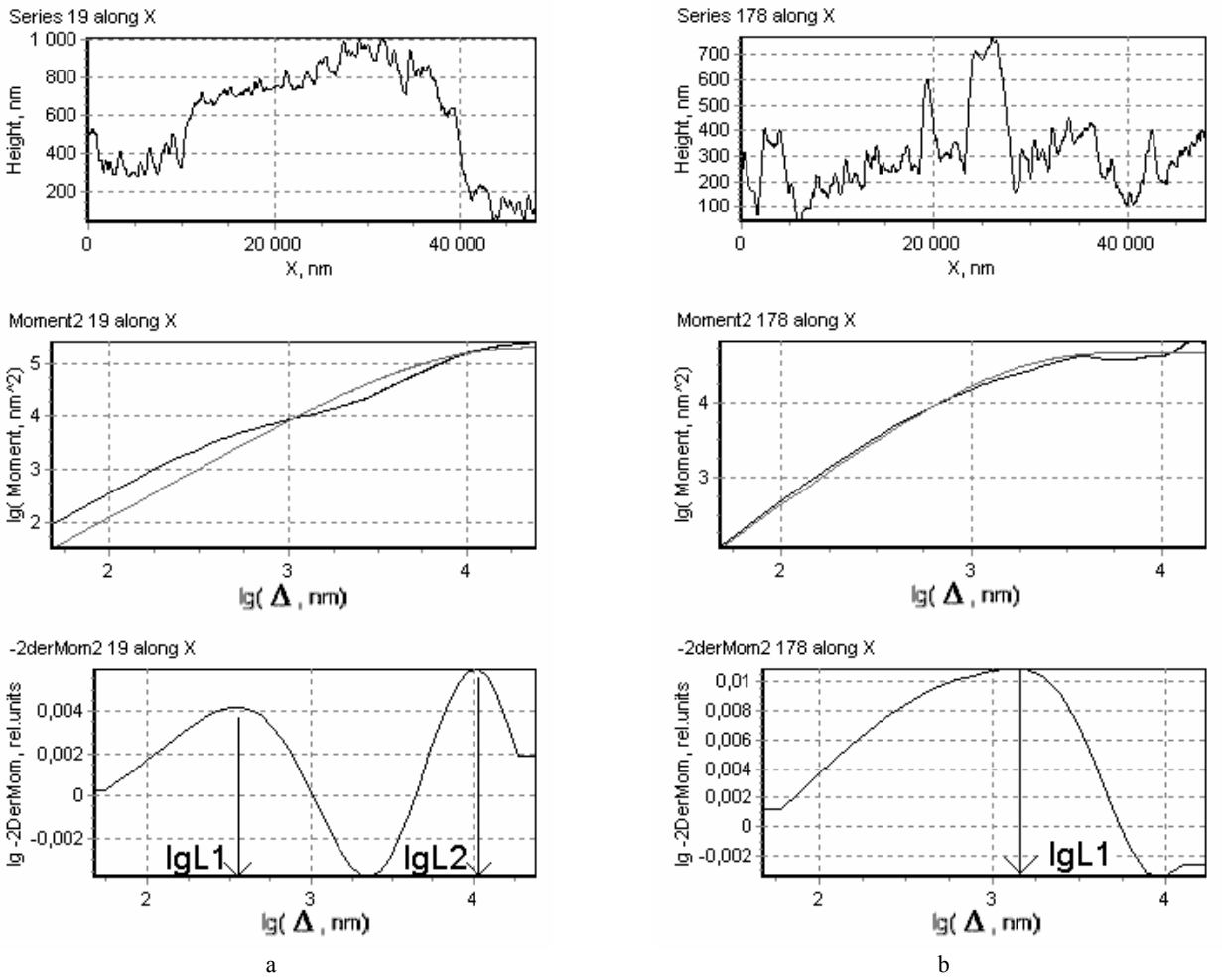

Fig. 2. Exemplification of the working principle of new procedure for two profiles (upper plots) of LiF dissolution surfaces, see below:

a – "old" procedure (see Appendix A) gives by SF (middle plot) of some real profile one effective CL 5.2 mcm. But new procedure (Appendix B) gives two CLs 0.34 mcm and 10.7 mcm corresponding to the "steps" of calculated SF and to two maximums of bottom plot – a negative second derivative of SF;

b – in the simplest case of only one CL (one "step") both procedures give close evaluations of its value 1.23 mcm and 1.21 mcm, see Fig. 1

DETERMINATION OF CORRELATION LENGTHS BY SF CURVATURES

The described above scheme of SF parameterization enables to determine only one CL. But real situations turn out to be more complex. For example, authors of [10] used SF approximation on the base of two similar terms with two sets of parameters in the brackets of eq. (A1, b), see eq. (C1), to parameterize the calculated SF with two "steps" (that implies a presence of two imposed processes in the case of temporal series [10]). This required to select seven parameters "by hands".

Automatic realization of such a procedure of selection of 6 – 7 parameters is a very complex problem. Therefore it was proposed to use evaluation of CLs by positions of SF curvature extremums. An algorithm of such a procedure is described in Appendix B (algorithm A2). Fig. 2 shows how new procedure works. It is seen that in the simplest case of presence of only one CL new procedure gives evaluation close to one obtained by "old" procedure.

Appendix C describes the checks of the proposed procedure on model SFs and structures. It demonstrates ability of new method to evaluate also the sizes (persistency lengths) of non-chaotic objects or geometrical forms if they will be registered in the surface structure of objects studied by SPM.

It should be noted that in spite of evident accomplishments of algorithm A1 as a computer based parameterization tool it has some demerits such as influence of SF order on result of CL determination, or dependence CL on maximum lag value, great calculation time expenses due to necessity to calculate gamma functions and their logarithms during iterations in CL selection. On the contrary, positions of the peaks of negative second derivatives (corresponding to CLs determined by new procedure) do not change with variation of SF order or its maximum lag. More over, new method requires one calculation of the first and second derivatives and it demands the calculation time expenses by (not lesser than) three orders lesser. On the other hand, although CLs are the most important physical parameters of chaotic series, but proposed procedure does not determine the other parameters as it was done in [10]. Automatic determination of all the parameters of complex approximations (like eq. (C1)) will require, probably, a "hybridization" of the both "old" and new algorithms. It should be noted also that besides negative second derivative other possibilities were investigated: the (first) curvature of SF (remind that first curvature of function $f(x)$ is $f''/(1+f'^2)^{3/2}$), inverse second derivative, ratio of the first derivative to the second one. The described version was found to be optimal due to a number of reasons (for example, minimum changeability of characteristics obtained for transition from some profile to its neighbor, H independent CL in model investigations, etc.).

APPLICATIONS TO REAL SPM DATA PROCESSING

The results described in this section were obtained in the same way. Fig. 2 gives the examples of views of SFs and their negative second derivatives that are more or less typical for all the experimental data that, of course, were different by their CLs values that range from several nanometers to tens of micrometers. In the following lets notation L1-0 ($=L_1$ in notations of Appendix A) be for correlation length determined on the base of trend (A1) [4 – 7], and L1, L2, etc. be the hierarchical correlation lengths (from smallest one to the greater one) determined by proposed method. Note that this method needs no theoretical speculations to deduce approximation model to fit the real SFs. It finds CLs directly from the data and the CLs determined can be used for further data processing.

A. LiF dissolution surfaces

An influence of hydrogen treatment (by digester at high temperature and pressure) on the dissolution surfaces of LiF monocrystals was studied in [5]. A mirror technique was used when monocrystal is cleaved into two pieces with mirror surfaces, then one piece is treated but the other is kept as a reference sample. Atomic force microscopy (AFM) data (contact mode, (50×50) mcm, (1000×1000) points) were obtained for the samples dissolved in the water at temperatures 25 °C – 50 °C. Two CLs were revealed, Fig. 3.

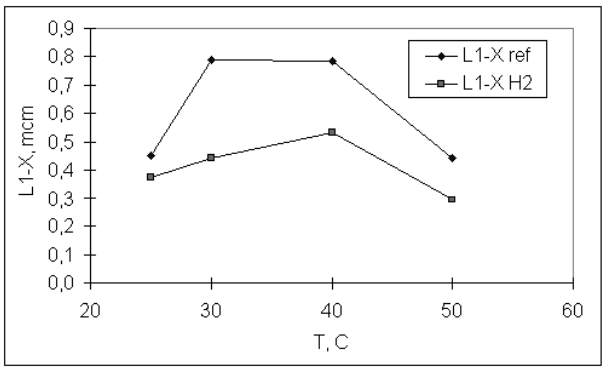

a

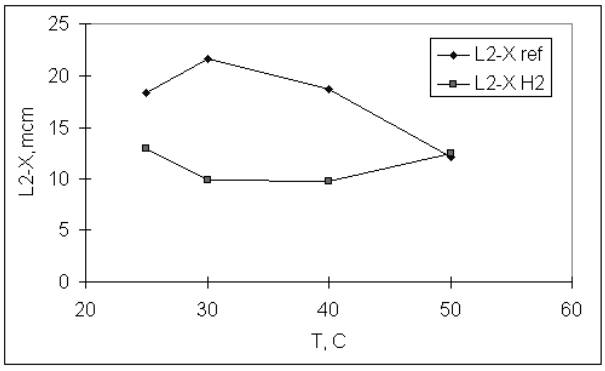

b

Fig. 3. Dependence of CLs L1 (a) and L2 (b) for AFM data of [5]. "ref" (reference) is for initial crystal, "X" is for the direction of picked up profiles. Increase in dissolution temperature diminished effect of hydrogen treatment on extrusion-intrusion heterogeneities. Each value was obtained by SF averaged over 200 randomly picked up profiles and by averaging over 3 – 5 relief images

The presence of two surface substructures is due to the way of monocrystal surfaces making – by cleavage

generating the multiple crystal defects due to shear stresses. CL L1 (300 nm – 800 nm) corresponds to the dislocation lodgments. CL L2 (10 mcm – 25 mcm) corresponds to extrusion-intrusion heterogeneities appearing as the "steps" and "crests" on dissolution surfaces [5]. Surface anisotropy is due to the latters.

In [5] the hydrogen treatment was revealed on the base of L1-0 (1 mcm – 4 mcm) only by its anisotropy (by the differences between the values determined for the "X" and "Y" directions that was 0.3 mcm – 3 mcm). Here we can register the hydrogen treatment effect directly by the values of CLs. Impregnation of monocrystal with hydrogen results in distortion of crystal lattice, increases its defect density, and so decreases the CLs. Effect of the hydrogen on surface anisotropy appears in the differences of greater CLs L2Y-L2X (8 mcm – 10 mcm).

It is seen also that the greater CLs of reference and treated samples vary in different ways with dissolution temperature increase. The CL L1-0 determined in [5] represents a "mixture" of the small and great CLs (see Fig. 2) but, nevertheless, was able to reflect the hydrogen treatment effect as an effective parameter reflecting anisotropy of dissolution surfaces.

B. Track-etched membranes

Recently, the results of AFM investigations of the track-etched membranes have been reported [6]. Track-etched membranes were produced of thin (10 mcm – 20 mcm) extrusion made films of poly(ethylene terephthalate) (PET) by irradiation by a flux of high-energy heavy multicharged ions (250 MeV, ^{84}Kr with a fluence varied from 10^6 to 10^9 ion/cm^2) with following etching in 1 mol/l NaOH solution. During etching the local regions (tracks) damaged by heavy particles become the pores. The film porosity can be controlled by irradiation time and particle flux density. This object is a proper test for new procedure as, although the characteristic geometrical objects – spherulites (about 50 nm in diameter) are easily identified on the PET surface, but the surface remains chaotic on the whole. So one can hope to determine the both "persistency length" (see Appendix C) corresponding to spherulites and CL corresponding to their surface organization.

AFM data [6] (tapping mode, (3×3) mcm, (1024×1024) points) processing enabled to reveale two CLs corresponding to two different scale levels of PET film surface organization, Fig. 4. The lowest CL L1 (35 nm – 50 nm) corresponds to spherulite size. This value increases with increase in porosity. CL L2 (1400 nm – 800 nm) reflects the size of the correlated PET surface regions – the groups of 1000 – 500 spherulites. This parameter decreases with increase in porosity. This tendency reproduces the L1-0 variation [6], but the latter, as far as we know now, was a "mixture" of two different CLs, see Figs. 2. Decrease in L2 and L1-0 can be interpreted as disordering of extrusion-made PET films surface due to its relaxation during irradiation and subsequent chemical etching. Variation of effective spherulite size L1 can be due to the both film surface heterogeneity on the whole and destruction and redistribution of amorphous shells of spherulites destructed by irradiation.

We can see that the smaller CL L1 corresponding to spherulites is almost the same for non-treated film, one etched without irradiation and the porous film with minimum porosity. But the greater CL L2 is influenced by irradiation. Taking into account that irradiation effects the L1 values of the films with greater porosity, we see that effect of irradiation on the PET films surface structure is non-trivial and requires further detailed investigation. The decrease in PET surface ordering with increase in porosity here is reflected by decrease in greater CL L2. In [6] this effect was reflected by "old" CL L1-0, Both the new L2 and "old" (effective) L1-0 parameters decrease approximately in two times for porosity increase from 0.2 to 6 %.

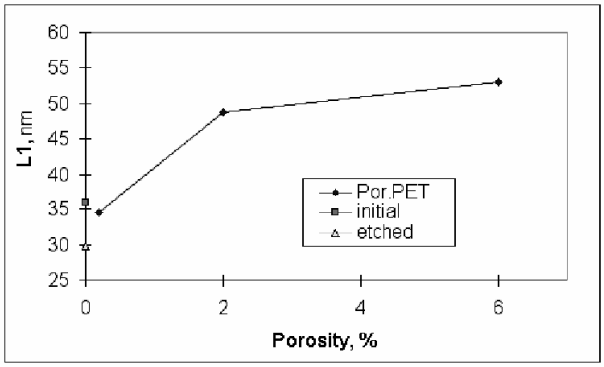

a

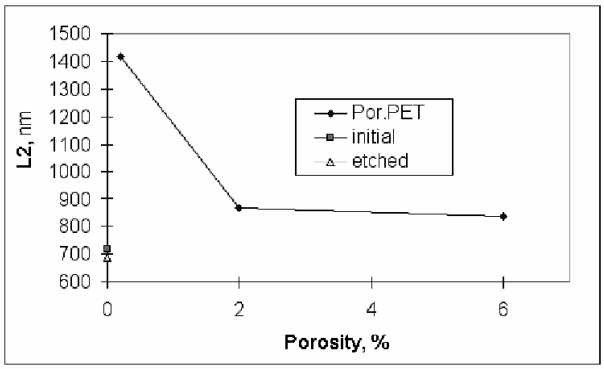

b

Fig. 4. Dependencies of CLs L1 (a) and L2 (b) on the PET film porosity for data of [6]. Each value was obtained by SF averaged over 200 randomly picked up profiles and by averaging over 5 – 16 relief images. "Por.PET" is for porous PET films, "initial" – for non treated PET film, "etched" – for etched PET film without irradiation

C. Shungite rocks

The new approach was applied to processing the AFM data obtained for finished surfaces of the samples of stratified shungite with various carbon contents [11, 12], see Table 1. Shungite is a natural carbon containing mineral with main components the carbon and silicates. The surface of shungite rock has mosaic structure with carbon and mineral areas due to a globular structure of the rock. Three scale levels of shungite structure organization were revealed.

The finished surfaces were investigated using SPM "Smena" (NT-MDT, Zelenograd Town) in tapping regime for the goals to obtain a distribution of phase shift of cantilever vibrations with respect to basic signal – a so

called phase contrast images. The phase shift is determined by a friction at cantilever tip and depends on both the local characteristics of material surface and height gradient. So the surface pieces images with local height gradient not greater than 0.03 (30 nm / 1 mcm) were selected for further processing among a lot the data obtained. Under this condition one can reasonably believe that the obtained data reflect the distribution of local hardness (and, subsequently, phase structure) of the surface in relative units. As far as the author can judge, such investigations were made at first.

As follows from data of Table 1, three levels of shungite structure were revealed that seem to be characteristic for stratified shungites at all [11]. The size L1 (several nm) responds to the pores. The sizes L2 (15 nm – 44 nm) and L3 (300 nm – 400 nm) respond to globules sizes. Calculation of SFs was conducted for maximum SF lag 50 % – 80 % of obtained surface piece image size 2 mcm and it was impossible to reveal the structural level at scale 1 mcm and greater.

Table 1. The results of phase shift distribution processing for (2 × 2) mcm (1024 × 1024 points) pieces of the finished surfaces of shungite rocks. L1, L2, L3 and L1-0 are the CLs each obtained by SF averaged over 200 randomly picked up profiles and by averaging over 5 –16 relief images. C is a carbon contents

Shungite type	C, %	L1, nm	L2, nm	L3, nm	L1-0, nm
Shun'ga	98	2.11	15.1	287	29.8
Zazhogino	60	4.56	30.8	395	34.7
Maxovo	30	5.78	44.1	366	20.6
Lidit	2	4.94	29.0	364	17.3

Analysis of the data for surface pieces (5 × 5) mcm reveals one more structural level at scale 1.5 mcm – 2.5 mcm. The greater scale the poorer its appearance statistics. So one can believe that shungite rocks are mostly uniform at the scales greater than 1.5 mcm. It should be noted that this conclusion is in agreement with results of [4] where the CL values 1.2 mcm – 1.4 mcm were obtained for finished shungite rocks (contact mode, (7 × 7) mcm, (1000 × 1000) points, using SF having one step processed by algorithm A1).

The globules of the sizes 15 nm – 39 nm were reported in [13] by the data obtained by contact AFM of cleavage shungite surfaces washed out in mixture ethanol-water in ultrasonic bath. The globules were revealed by visual analysis of (0.35 × 0.35) mcm surface pieces. Such a technique of sample preparation can destruct the traces of smaller objects. The roughness of the cleavage surfaces did not enable to investigate surface pieces greater than (0.5 × 0.5) mcm to reveal the globules of the greater size. So the AFM technique proposed in this work is more proper for the goals of revelation of the structural levels in the wide rage of scales.

CONCLUSIONS

A generalized approach proposed in this work for determination of correlation lengths of the surface profiles on the base of structural functions processing gives the adequate evaluations of characteristic sizes of the elements and substructures of real surface structures presented by SPM data. The use of the set of correlation lengths instead of one effective length makes it is possible to analyze in details a hierarchical structure of the objects under study. This is extremely important for investigation of natural objects with complex many level structures, in analysis of physical consistent patterns and processes due to the structure. The described examples of real structures processing were selected as the examples of the systems of various physico-chemical nature (monocrystal before and after saturation with hydrogen, amorphous-crystalline (porous) polymer film and natural rock). The proposed approach enables to identify two (as a minimum) scale levels of structural organization of the surface in these different systems. The method can be used with all the types of SPM data.

Thus the proposed method provides adequate evaluation of both the correlation lengths in the case of chaotic structures and the characteristic sizes ("persistency lengths") in the case of the structures with characteristic elements that can be interpreted in the special or geometrical terms.

APPENDICES

A. Algorithm A1 of determination of the parameters of SFs of real profiles on the base of non-linear approximation [4 – 7]

In [3, 9] it was proposed to approximate SF by formula

$$\Phi^p(\Delta) \approx G_1(p)\cdot\sigma^p\cdot\left[1-\Gamma^{-1}(H)\Gamma(H,\Delta/L_1)\right]^p \quad \text{(A1, a)}$$

or

$$\Phi^p(\Delta) \approx G_1(p)\cdot\left[\sigma\gamma(H,\Delta/L_1)/\Gamma(H)\right]^p . \quad \text{(A1, b)}$$

Here $G_1(p)$ is a numeric coefficient (for SF of the second order, $p = 2$, its theoretical value is $G_1(2) = 2$), σ is a standard deviation of the profile, H is a Hurst exponent, L_1 – CL.

$\Gamma(H) = \int_0^\infty e^t t^{H-1} dt$ – gamma function,

$\Gamma(H,z) = \int_z^\infty e^t t^{H-1} dt$ – incomplete gamma function (the first one),

$\gamma(H,z) = \int_0^z e^t t^{H-1} dt = \Gamma(H) - \Gamma(H,z)$ – incomplete gamma function (the second one).

For the small values of the SF lag, i.e. for $\Delta/L_1 = z \to 0$, the gamma function can be expressed as

$$\gamma(H,z) = \int_0^z e^t t^{H-1} dt \approx z e^{z/2} (z/2)^{H-1} .$$

Then for $\Delta \to 0$ the SF is

$$\Phi^p(\Delta) \approx G_1(p)\cdot\sigma^p\cdot e^{p\Delta/(2L_1)}\left(\frac{\Delta}{L_1}\right)^{Hp}\frac{1}{[\Gamma(H)]^p 2^{H-1}} \propto \left(\frac{\Delta}{L_1}\right)^{Hp}. \quad \text{(A2)}$$

Linear regression in double logarithmic axes of the dependence $\Phi(p)(\Delta)$, i.e. of the dependence $\ln[\Phi_{(p)}(\Delta)]$ on $\ln[\Delta]$, for a small number of the fist points, for example,

three) gives declination value *Hp*. Determining this declination and dividing it by SF order value *p* we obtain Hurst parameter *H*. Scheme of parameterization of SF of the second order is shown in Fig. 1. Parameter L_1 was calculated by a special algorithm A1.

The algorithm consists of selection of L_1 value in SF approximation by condition of coincidence of the slope of linear regression in double logarithmic coordinates (LRDLC) of the calculated SF with given order SF *p*.

Calculated SF of order *p* is processed in the form of sets of coordinates (lags) $X = \{\Delta_1, \Delta_2, ..., \Delta_N\}$ and the corresponding function values $Y = \{y_1, y_2, ..., y_N\}$. At the first step the value *pH* is determined by LRDLC method of the first 3 – 5 points of SF, i.e. as the slope of lg*Y* via lg*X* dependence. Then dividing this value by order *p* one can obtain evaluation of Hurst parameter *H*.

At the second step a value $L_1 = \Delta_1$ is set and the set $G(H, L_1) = \{g_1, g_2, ..., g_N\}$, $g_k = \gamma(H, \Delta_k / L_1)$ is calculated. Setting the variation of L_1 δL_1 (usually equal to discretization step of theset *X*) and calculating the slope *P* by LRDLC of the sets *Y* and *G*. one obtains the initial conditions for iterative selection of L_1.

The algorithm to calculate slope $p1$ of LRDLC for the sets *Y* and $G(H, L_1)$:

if $P > p$: if $p1 > p$, then to increase L_1 by δL_1;

if $p1 < p$, then to decrease L_1 by δL_1, decrease δL_1 in 10 times, to increase L_1 by δL_1;

if $P < p$: if $p1 < p$, then to increase L_1 by δL_1;

if $p1 > p$, then to decrease L_1 by δL_1, decrease δL_1 in 10 times, to increase L_1 by δL_1;

Repeat (*) while $|p - p1| > 0{,}001$ or $L_1 < \Delta_N$.

If $L_1 < \Delta_N$, then to find $L_1 = \Delta_k$, which minimizes variation of the slope $p1$ of LRDLC of the sets *Y* and $G(H, L_1 = \Delta_k)$ from the given value of SF order *p*. The constant $G_1(p)$ is calculated on the base of determined parameters and mean squared profile deviation σ by the formula

$$G_1 = \exp\left(\frac{Q}{N}\right) \Big/ \left(\frac{\sigma}{\Gamma(H)}\right)^{p1}, \quad Q = \sum_{k=1}^{N} \ln\left(\frac{y_k}{\gamma(h, \Delta_k / L_1)^{p1}}\right).$$

The output of the algorithm is a set of parameters *H*, L_1, $p1$, G_1. The quality of the approximation is determined by difference of the calculated SF order $p1$ and the given order *p*. The gamma functions are calculated on the base of recursive procedures and effective series.

B. Algorithm A2 of determination of the set of correlation lengths by curvature of calculated SF

The algorithm consists of determination of the positions of maximums of negative second derivative of SF in the regions with positive first derivative. Unnecessary operation is given in square brackets. Calculated SF of order *p* is processed in the form of sets of coordinates (lags) $X = \{\Delta_1, \Delta_2, ..., \Delta_N\}$ and the corresponding function values $Y = \{y_1, y_2, ..., y_N\}$.

- Dependence *Y*(*X*) with constant step along *x* is recalculated into dependence with constant step over lg(*x*) by linear interpolation using a set step over logarithmic scale. The number of points can decrease in 5 – 20 times;
- Dependence *Y*(*X*) [lg*Y*(lg*X*)] is smoothed;
- A set $Y'' = \{-([\lg]y_{k+1} + [\lg]y_{k-1} - 2[\lg]y_k)\}_{k=2,...,N-1}$ is calculated (the negative second derivative);
- Dependence *Y''*(*X*) is smoothed;
- The positions *L*1, .., *L*M of the first *M* (from 2 to 7) maximums of *Y''*(*X*) dependence are determined under condition of positive first derivative. These positions are the output of the algorithm.

Smoothing is done on the base of the simplest difference scheme of heat conductivity (diffusion) equation solution with constant boundary conditions. The proposed technique demands a number of operations lesser by three orders (and more) then algorithm A1. Discretization step (usually the parts of $\lg\Delta_1$) of logarithmic SF at the first stage influences the sensitivity of the algorithm to the presence of "steps" or resonance cauldrons of SF. The problem of sensitivity selection is solved by primary analysis of several variants of SF processing for randomly picked up profiles.

C. Checks of proposed procedure on model SFs and structures

First, new procedure was checked out for correctness of CL determination in the case of SF via eq. (A1). SF was plot by $L_{max} = 500$ points for the different Hurst parameters *H* and CL L_1 (in points number) for the order *p* values from 1 to 10, $G_1\sigma^p = 1$. An example of such model curve is shown in Fig. C1.

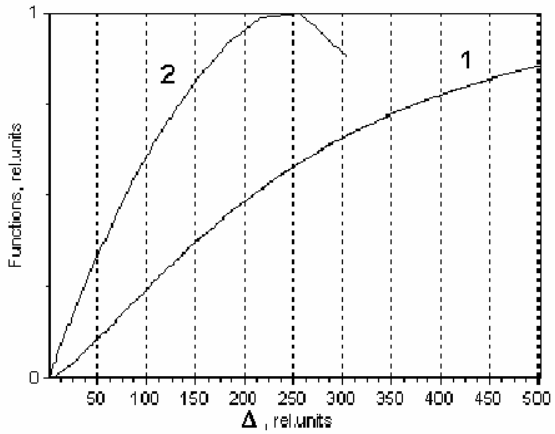

Fig. C1. Model SF plot by eq. (A1) for $p = 2$, $H = 0{,}7$, $L_1 = 250$, $G_1*\sigma^2 = 1$ (1), and its negative second derivative obtained by algorithm A2 (2). The curves are normalized by unit for convenience

The ratios L_1*/L_1 of CL calculated by algorithm A2 to given CL by which model SF was calculated are given in Table C1. It is seen that determination accuracy is 1 % – 2 % under condition that the set CL and *H* are not very small (in real cases *H* is less than 0.5 very rarely). It should be stressed that determined CL value L_1* is independent of the order *p* of model SF. The investigations with this model curve were the very base for algorithm A2 elaboration.

Test of algorithm A2 in the case of two "steps" was conducted using the model corresponding to complex SF approximation from [10] on the base of formula

$$\Phi^p(\Delta) \approx G_1(p) \cdot \sigma_1^p \cdot \left[\frac{\gamma(H_1, \Delta / L_{1-1})}{\Gamma(H_1)} + \frac{\alpha\sigma_2}{\sigma_1} \frac{\gamma(H_2, \Delta / L_{1-2})}{\Gamma(H_2)}\right]^p. \quad \text{(C1)}$$

Table C1. The ratios L_1^*/L_1 of CL L_1^* calculated by algorithm A2 to given CL L_1 by which the model SF was calculated for $p = 2$ and different H and ratios L_1/L_{max}

H	L_1/L_{max}				
	0.1	0.25	0.4	0.7	0.9
0.1	0.905	0.724	0.806	0.975	0.975
0.2	0.905	1.024	0.806	0.994	0.994
0.3	1.280	1.024	1.016	0.994	0.994
0.4	1.280	1.024	1.016	0.994	0.994
0.5	1.280	1.024	1.016	0.994	0.994
0.6	1.280	1.024	1.016	0.994	0.994
0.7	1.280	1.024	1.016	0.994	0.994
0.8	1.280	1.024	1.016	0.994	0.994
0.9	1.280	1.024	1.016	0.994	0.994
1.0	1.810	1.024	1.016	0.994	0.994

Fig. C2 shows this model curve and its negative second derivative. The parameters were chosen in such a way to reproduce the relations between parameters in [10] for the function plot by 1000 points with discretization step 1 nm.

As is seen from Fig. C2, algorithm A2 gives the satisfactory evaluations of a set of model CLs. The errors of CLs determination are due to discretization of logarithmic SF and effect of the term with greater SL on the curvature of the first (small) "step". This systematic error of small CL determination should be taken into account when using approximation (C1) on the base of CLs determined by algorithm A2.

Additional model investigations were carried out with model "surfaces" of two types: the surfaces with additive:

$$h(x,y)=A*(\cos((x-x0)*2\pi/T1/)+\cos((y-y0)*2\pi/T1))+ +A*(\cos((x-x0)*2\pi/T2)+\cos((y-y0)*2\pi/T2))+ +A*(\cos((x-x0)*2\pi/T3)+\cos((y-y0)*2\pi/T3)), \quad (C2)$$

and multiplicative imposition of harmonic vibrations (waves):

$$h(x,y)= A*(\cos((x-x0)*2\pi/T1)+\cos((y-y0)*2\pi/T1))* *(\cos((x-x0)*2\pi/T2)+\cos((y-y0)*2\pi/T2)* *(\cos((x-x0)*2\pi/T3)+ \cos((y-y0)*2\pi/T3)). \quad (C3)$$

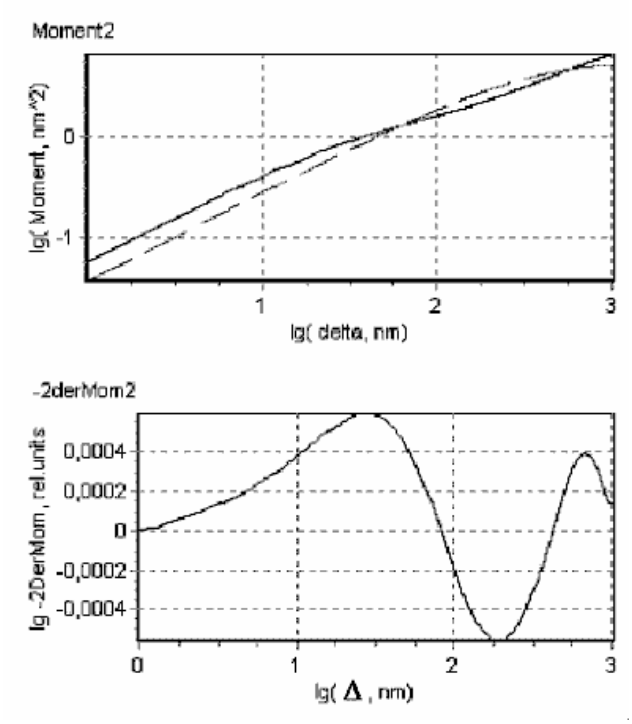

Fig. C2. Model SF (upper plot) by eq.(C1) for $p = 2$, $G_1*\sigma_1^2 = 1$, $H_1 = 0.45$, $L_{1\text{-}1} = 33$ nm, $H_2 = 1.0$, $L_{1\text{-}2} = 661$ nm, $\alpha\sigma_1/\sigma_2 = 2$, and its negative second derivative obtained by algorithm A2. Positions of bottom curve maximums correspond to CLs $L_{1\text{-}1} = 26.9$ nm, $L_{1\text{-}2} = 664$ nm. Approximation on the base of eq. (A1) gives "mixed" CL $L_1 = 364$ nm

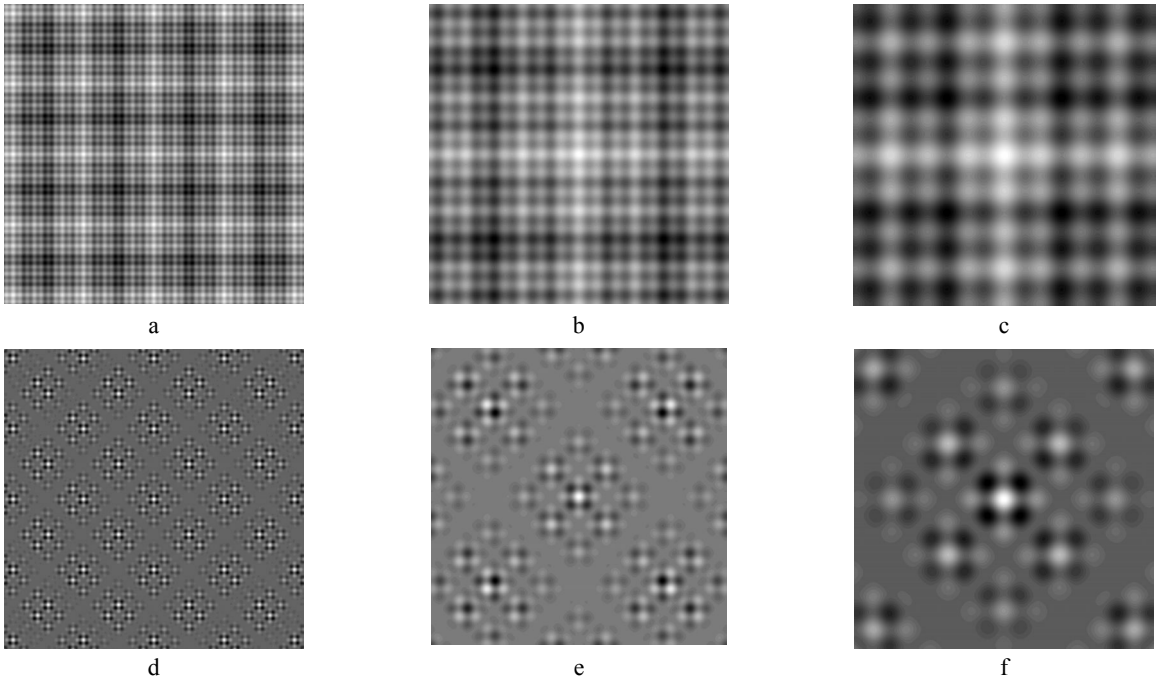

Fig. C3. The examples of surfaces (C2) (upper raw a, b, c) and (C3) (bottom raw d, e, f) in the form of grayscale images (1024 × 1024) nm with period T2 (from left to right) 80, 200, 400 nm

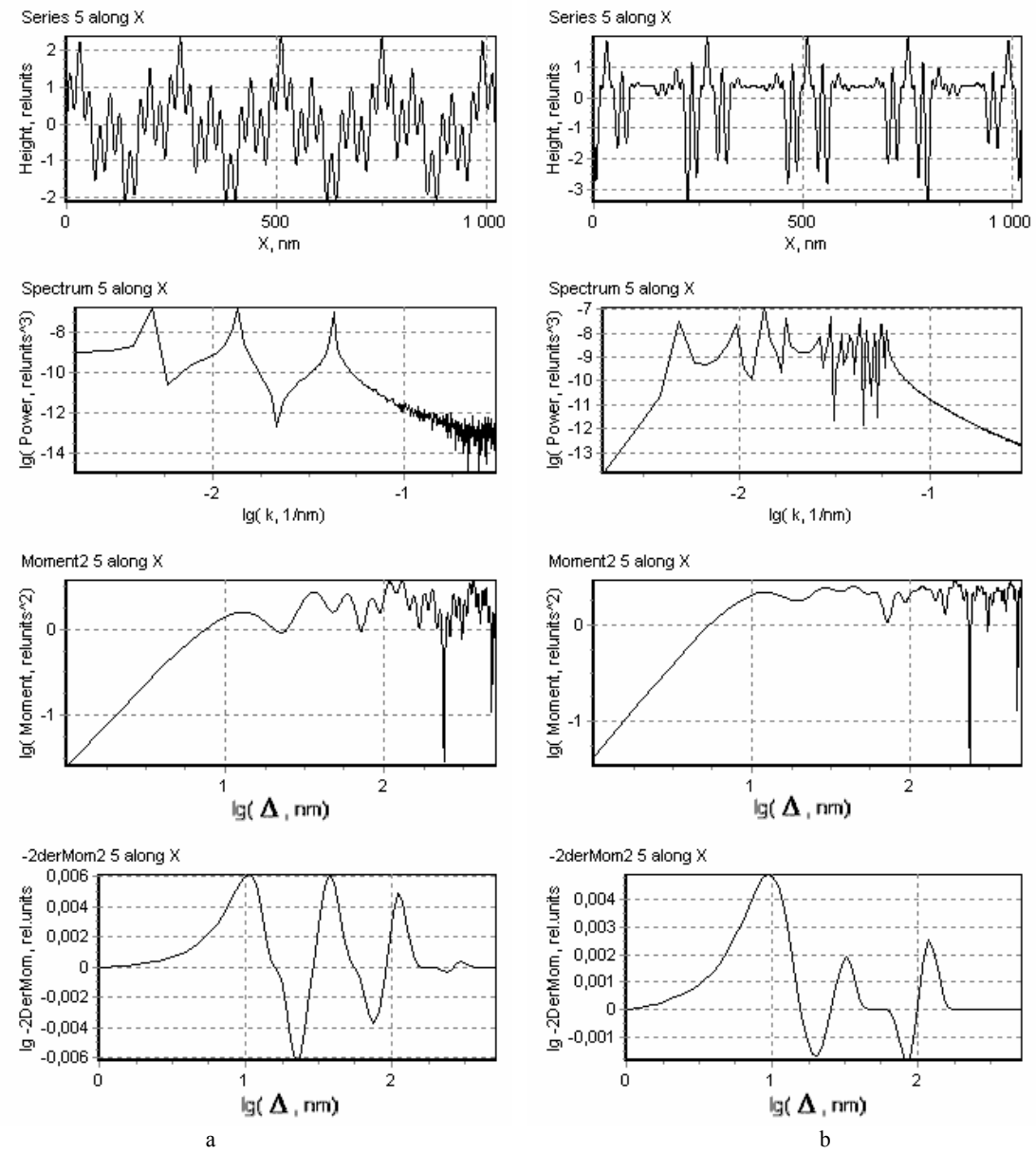

Fig. C4. Examples of the profiles, power spectrums, SFs and their negative second derivatives by algorithm A2 for additive (a) and multiplicative (b) surface structures for $T2 = 80$ nm

Here $h(x,y)$ is a relief height at the point (x,y), $T1$, $T2$, $T3$ – the periods, A – amplitude, $(x0, y0)$ – position of relief center. $T1/T2 = T2/T3 = \pi$. A random noise with amplitude $0.02A$ was imposed on the surfaces to prevent zero values of SF at inevitable resonance caldrons. The examples of such surfaces are given in Fig. C3. Their typical profiles, calculated spectra, SFs and their negative second derivatives are shown in Fig. C4.

The results of processing the series of these model surfaces with period $T2$ from 40 nm to 400 nm are shown in Figs. C5, C6. The proposed algorithm A2 determines presence of three CLs (here the "persistency lengths") in each case. Their ratios vary near π value which was introduced in the models. In this case of imposition of harmonic waves the parameters $L1$, $L2$, $L3$ give a good evaluation of the halves of corresponding periods (the proportionality coefficients of the linear trends of $L2(T2)$ dependences are about 0.5). This consistent pattern is more valid for additive structure. Note that in this case algorithm A2 is able to reveal not the "steps" but resonance structure of SF even in the case of multiplicative structure.

A non-trivial fact is a differentiation of the three levels of the structure for the both additive and multiplicative types. It should be noted that if in the case of additive structures we can identify three harmonic components by three peaks of Fourier power spectra of surface profiles (the peaks are fuzzy due to noise imposed), but in the case of multiplicative structures such an identification is problematic, Fig. C4. However, algorithm A2 enables to do this. Using the power spectrums and SFs together (as it does in FNS in general) one can identify both the presence of substructure scale levels and type of the structure (additive or multiplicative). From Figs. C5, C6 it is also seen that algorithm A1 gives only evaluation of the minimal CL.

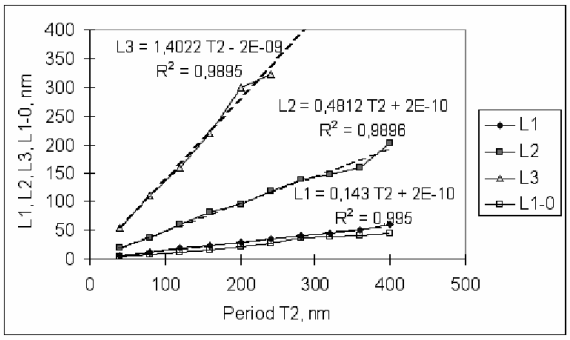

a

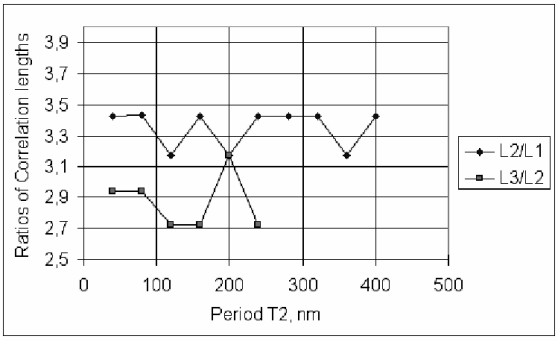

b

Fig. C5. Dependences of CLs (or "persistency lengths") *L*1-0 (determined by A1) and *L*1, *L*2, *L*3 (determined by A2) (a) and their ratios (b) on the value of "middle" period T2 for additive model surface (C2). SFs of the second order were calculated. The ratios of proportionality coefficients of linear trends are 2.91 (*L*3/*L*2) and 3.37 (*L*2/*L*1)

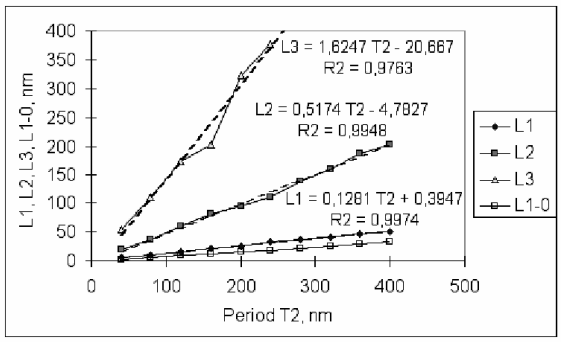

a

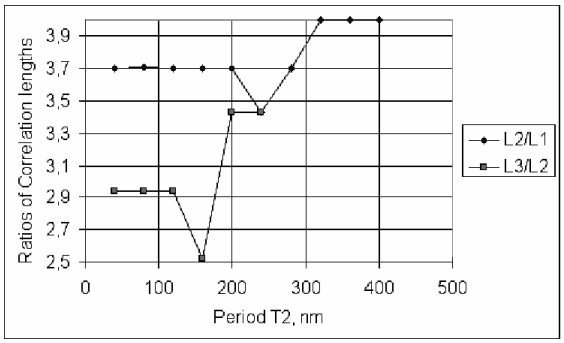

b

Fig. C6. Dependences of CLs (or "persistency lengths") *L*1-0 (determined by A1) and *L*1, *L*2, *L*3 (determined by A2) (a) and their ratios (b) on the value of "middle" period T2 for multiplicative model surface S2. SF of the second order were calculated. The ratios of proportionality coefficients of linear trends are 3.14 (*L*3/*L*2) and 4.04 (*L*2/*L*1)

Acknowledgments

This work was supported by RFBR Grant 04-02-16850. The author is grateful to Prof. S. F. Timashev (for 5 hours long discussion that stimulated introduction of the term "Persistency length" and model example in Fig. C2, eq.(C1)), Dr. A. B. Solovieva and Dr. V. A. Timofeeva (for granting the AFM data on track-etched membranes for calculations), Dr. N. N. Rozhkova (for granting the specimens of shungite rocks).

REFERENCES

1. **Magonov, S. N., Whangbo, M.-H.** Surface Analysis with STM and AFM. Weinheim; New York, Basel, Cambridge, Tokyo: VHC, 1996.
2. **Kiely, J. D., Bonnell, D. A.** Quantification of Topographic Structure by Scanning Probe Microscopy *J. Vac. Sci. Technol.* B, 15 (4) 1997: pp. 1483 – 1493.
3. **Timashev, S. F., Bessarabov, D. G., Sanderson, R. D., et al.** Description of Non-regular Membrane Structures: a Novel Phenomenological Approach *J. Membrane Sci.* 170 (2) 2000: pp. 191 – 197.
4. **Vstovsky, G. V., Solovieva, A. B., Kedrina, N. F., Timofeeva, V. A., Kalinin, Yu. K., Rozhkova, N. N.** An Atomic-force Microscopy in the Analysis of Composites Structure *Russian J. Phys. Chem.* 75 (11) 2001: pp. 1958 – 1961.
5. **Letnikova, A. F., Vstovsky, G. V., Timashev, S. F.** Formation of Anisotropic Fractal Structures during Dissolution of LiF Monocrystals *Materials Science* (*Medžiagotyra*) 7(2) 2001: pp. 98 – 103.
6. **Solovieva, A. B., Timofeeva, V. A., Erina, N. A., Vstovsky, G. V., Krivandin, A. V., Shatalova, O. V., Apel', P. Yu., Mchedlishvili, B. V., Timashev, S. F.** Peculiarities of the Formation of Track-Etched Membranes by the Data of Atomic Force Microscopy and X-ray Scattering *Colloid Journal* 67 (2) 2005: pp. 217 – 226 (Translated from *Kolloidnyi Zhurnal* 672 2005: pp. 248 – 258).
7. **Solovieva, A. B., Vstovsky, G. V., Kotova, S. L., Glagolev, N. N., Zav'yalov, S. A., Belyaev, V. E., Erina, N. A., Timashev, P. S.** The Effect of Porphyrin Supramolecular Structure on Singlet Oxygen Photogeneration *Micron* 36 2005: pp. 508 – 518.
8. **Frisch, U.** Turbulence. The Legacy of A. N. Kolmogorov. Cambtidge Univ. Press, 1995.
9. **Timashev, S. F.** Concept of Randomness in Chemistry and Ambiguity in the Results of Chemical Experiments *Theoretical Foundations of Chemical Engineering* 34 (4) 2000: pp. 301 – 314.
10. **Parkhutik, V. P., Timashev, S. F.** Informative Essence of Noise: New Findings in Electrochemistry of Silicon *Russian J. Electrochem.* 36 (11) 2000: pp. 1221 – 1235 (Translated from *Electrochimiya* 36 (11) 2000: pp. 1378 – 1394).
11. Shungite – a New Carbon-containing Raw Material. Eds. **Sokolov, V. A., Kalinin, Yu. K., Dyukkiev, E. F.** Petrozavodsk, Karelia, 1984 (in Russian).
12. **Melezhik, V. A., Fallick, A. E., Filippov M.M., Larsen O.** Karelian Shungite – an Indication 2.0-Ga-old metamorphosed Oil-shale and Generation of Petroleum: Geology, Lithology and Geochemistry *Earth-Science Reviews* 47 1999: pp. 1 – 40.
13. **Golubev, E. A.** Supramolecular Nanostructures in the Natural Non-crystalline Substances by the Data of Scanning Probe Microscopy *Proc. Conf. "Probe Microscopy 2000"* N. Novgorod, IPM RAS, 2000: pp. 97 – 102.

DOI: 10.5755/j02.ms.26442